Development of a three-dimensional model of lung cancer using cultured transformed lung cells

Article *in* Cancer biology & therapy · March 2009

Impact Factor: 3.07 · DOI: 10.4161/cbt.8.4.7432 · Source: PubMed

8 authors, including:

Thomas J Goodwin
Sovaris Aerospace (consulting)
57 PUBLICATIONS **1,822** CITATIONS

[Cancer Biology & Therapy 8:4, 356-365; 15 February 2009]; ©2009 Landes Bioscience

Research Paper

Development of a three-dimensional model of lung cancer using cultured transformed lung cells

Roger A. Vertrees,[1,*] Maureen McCarthy,[4] Travis Solley,[1] Vselovod L. Popov,[2] John Roaten,[3] Matthew Pauley,[3] Xiaodong Wen[1] and Thomas J. Goodwin[5]

Departments of [1]Surgery, [2]Pathology; and the [3]School of Medicine; University of Texas Medical Branch; Galveston, TX USA; [4]University Space Research Association; [5]Disease Modeling/Tissue Analogues Laboratory; NASA Johnson Space Center; Houston, TX USA

Abbreviations: 3-D, three-dimensional; ML, monolayers; HBTC, human mesenchymal bronchial-tracheal cells; FBS, fetal bovine serum; HBTC, human bronchial tracheal cells; RWV, rotating walled vessel; CMF-PBS, calcium- and magnesium-free phosphate-buffered saline; IHC, immunohistochemistry; TEM, transmission electron microscopy; NHBE, normal human bronchial epithelial; HBE, human broncho-epithelial

Key words: tissue engineering, lung cells, three-dimensional culture

Despite great strides in understanding cancer biology, the role cellular differentiation and three-dimensional (3-D) structural organization play in metastasis and malignancy remains unclear. Development of 3-D cultures may ultimately provide a model facilitating discovery and interpretation of more relevant information for the expression and role of antibodies in lung cellular pathobiology. The purpose was to develop traditional monolayer (ML) and 3-D cultures of a known transformed metastatic lung cell line and then determine similarities and differences between cultures in terms of differentiation, molecular marker expression and metastasis. A transformed lung cell line (BZR-T33) was initially transfected with green fluorescent protein (GFP) in ML culture. Nude mice were inoculated with BZR-T33 and observed for metastasis. BZR-T33 was grown as ML and 3-D cultures under identical conditions. Immunohistochemical comparison for degree of antibody expression between cultures and control tissue were studied. Electron microscopy (EM) for identification of ultra structures was done and compared between cultures. A 3-D co-culture containing GFP-transformed cells over an immortalized lung-cell line was developed. The GFP-transfected cell line formed tumors and metastasized in mice. EM identified significant mitochondrial and granular endoplasmic reticular pathology in ML not seen in 3-D. Degree of differentiation shows ultra structures and antibody expressions were more representative of control tissue in 3-D than ML. The co-culture experiment in 3-D demonstrates the ability of transformed cells to penetrate the sub-layer of immortalized cells. Development of 3-D cultures will provide a new and powerful tool to study lung biology and pathobiology.

*Correspondence to: Roger A. Vertrees; Department of Surgery; University of Texas Medical Branch; 301 University Boulevard; Galveston, TX 77555 USA; Tel.: 409.772.8629; Fax: 409.772.1421; Email: rvertree@utmb.edu

Submitted: 06/25/08; Accepted: 11/17/08

Previously published online as a *Cancer Biology & Therapy* E-publication: www.landesbioscience.com/journals/cbt/article/7432

Introduction

Current lung-cancer models consist of cell culture, organ cultures,[1,2] transgenic mouse models[3] and xenotransplants to immune compromised mice.[4] None of these accurately predicts events in vivo. At the molecular level, cultured cells grown in the traditional manner differ widely in their expression of differentiated markers, adhesion receptors and growth factor receptors compared to cells in situ.[5] Organ cultures, while informative and a step closer, still lack the reliability necessary to predict clinical correlates.[6] Current animal models of lung cancer consist mainly of models of animal cancer or as a host for human cancers, again with unreliable clinical correlations. It will continue to be difficult to make any firm statement relating events in cell culture to human cancer pathobiology with a high degree of fidelity until a model is developed that addresses three-dimensional (3-D) architecture and cellular differentiation.[3,7,8]

Three-dimensional (3-D) tissue culture models have become an increasingly valuable tool in tumor biology; increasing our understanding of homeostasis, cellular differentiation and tissue organization.[9] Three-dimensional cultures can be formed in one of two ways: as an organ culture or as an aggregate of cells. Organ cultures are propagated from tissue fragments,[1,10] whereas aggregates are tissue cultures engineered in three dimensions.[11-15] A technology developed at NASA's Johnson Space Center[16] that includes horizontally rotating cylindrical tissue culture vessels, a solid matrix, and co-cultivation of epithelial and mesenchymal cells is being studied for its potential contribution to lung cancer. Goodwin and associates have reported on its application in ovarian,[11] prostate[17] and colon[16] cancers.

We recently reported on the development of a 3-D model using an immortalized human lung cell line and show that differentiation expressed in the 3-D culture more closely approximates that seen in normal human lung explants than in traditional monolayer cell cultures. Additionally, we were able to document by electron microscopy the presence of lipid bodies, microvilli and tight junctions in the 3-D cultures not seen in monolayer preparations.[5]

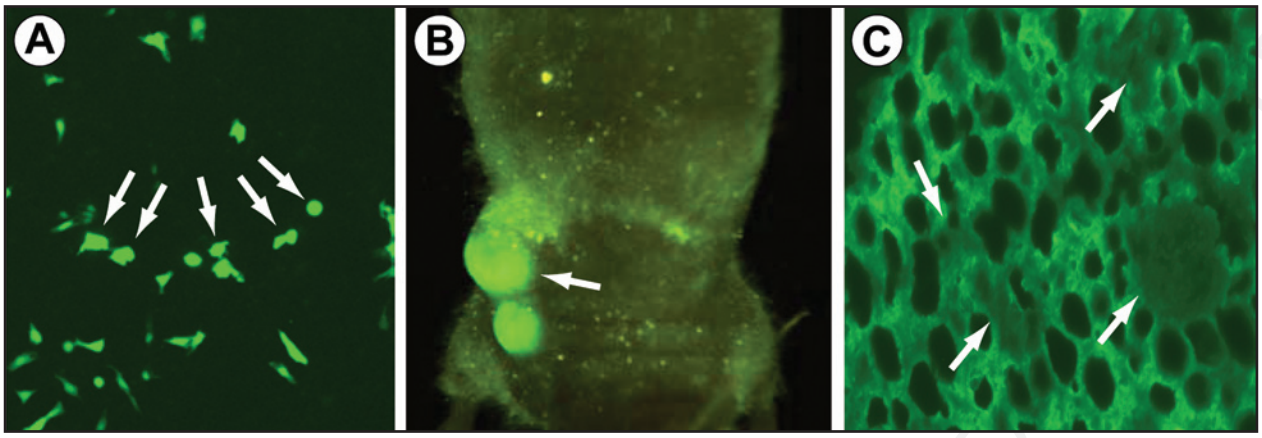

Figure 1. Green fluorescent protein transfected cells (→). (A) Presence in traditional monolayer cell cultures. (B) Two weeks after a supraclavicular injection. Green fluorescence is proof of metastasis. (C) Lungs removed at necropsy, green fluorescence demonstrates the metastasis of these cells.

The goal for the present research was to study the difference in antibody expression and ultrastructure when a known transformed lung cell line was grown in both 2-D and 3-D environments. We report our achievements constructing these 3-D cell cultures that use primary human mesenchymal bronchial-tracheal cells (HBTC) as the foundation matrix, and a transformed adult human bronchial epithelial immortalized cell line (BZR-T33).[18-20] Cells grown under these conditions have demonstrated aspects of differentiation and metastasis more closely related to cells grown in situ rather than those in traditional monolayers (MLs) or as floating suspensions.

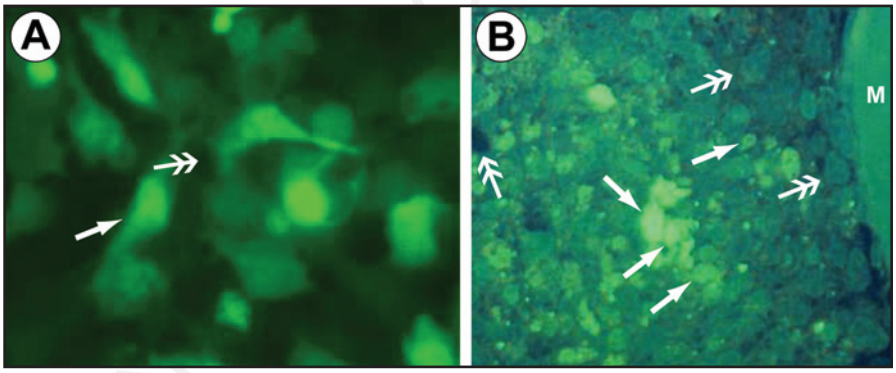

Figure 2. Green fluorescent protein transfected cells in culture. (A) A mixed 2-D culture of BEAS2-B and BZR-T33-GFP cells. The BZR-T33-GFP cells are detected by the green fluorescence (→) the unstained BEAS2-B cells (←). (B) Shows a culture of BZR-T33-GFP cells (→) over a co-culture of BEAS2-B cells (←). Note the penetration of the BZR-T33-GFP cells (→) into the BEAS2-B (b arrow) under layer. The microcarrier is also visible on the right.

Results

GFP experiments. In these experiments BZR-T33 cells were transfected with green fluorescent protein. A positive or transfected cell will appear green whereas those that were not transfected display a lack of color. Figure 1 is included in order to demonstrate the metastatic potential of the BZR-T33 cell line was not affected by the transfection of GFP. Figure 1A shows a traditional monolayer cell culture that included both BEAS2-B and BZR-T33-GFP (←) cells. Figure 1B shows a mouse two weeks after a supraclavicular inoculation of BZR-T33-GFP cells (←). These cells formed a subcuticular tumor as shown in Figure 1B. Also many metastatic foci can be identified. Figure 1C is fluorescence photograph of a lung removed from one of the nude mice that received the BZR-T33-GFP (←) inoculation. The green fluorescence indicates the metastatic potential of the BZR-T33-GFP cells which shows that these cells have invaded lung parenchymal tissue.

Figure 2A, BZR-T33-GFP (←) cells were grown as a traditional monolayer with unstained BEAS2-B cells («). The BZR-T33-GFP cells are detected by the green fluorescence (←). Figure 2B shows a mixed co-culture of BZR-T33-GFP cells over a co-culture of BEAS2-B cells (unstained). Note the penetration of the BZR-T33-GFP cells (←) into the BEAS2-B (« under layer. The microcarrier (M) is also visible.

Electron microscopy. In the traditional 2-D cultures, cells appear as individual cells with limited interactions (Fig. 3B). In 3-D culture, normal BZR-T33 (Fig. 3B) cells form tight junctions and complexing between two cell-covered microcarriers in which the cells are able to communicate. These cellular interactions are not visible in Figure 3A cells grown as monolayers, thus providing evidence that sustains the self ordering seen in the these cultures. Three-D cells show cytoplasm full of ribosomes (hence lighter in density) with a few cisterns of granular endoplasmic reticulum and some mitochondria. This data provides evidence for the differentiation that occurs when transformed lung cells are grown in 3-D cultures.

Human lung immunocytochemistry. Samples were collected at intervals across the initial growth experiment and prepared for IHC as previously outlined. Graded results appear in Table 2.

Markers of cell-to-cell junctions. ZO-1 (Fig. 4), a measure of tight junctions found on perimeters of polarized epithelium was surveyed to illuminate intercellular communications and cellular polarity. The normal human lung sample is provided as a control and for comparison between the two samples and shows a positive response at the apical membrane. The only positive staining for ZO-1 is seen in the 3-D specimen (BZR-T33) as a brown color on the cell surface.

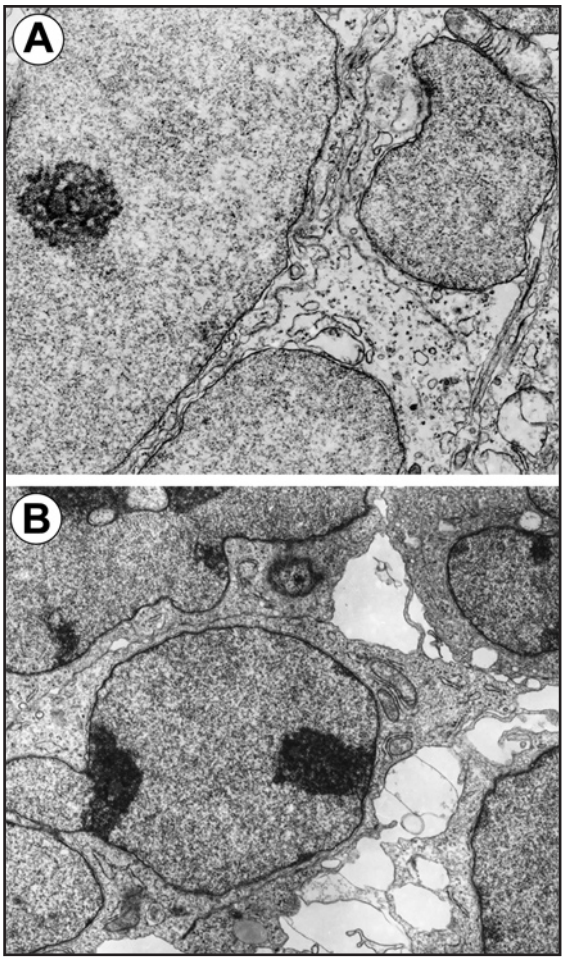

Figure 3. Electron microscopy comparisons between 2-D and 3-D cultures. (A) (2-D) demonstrates cells with swollen mitochondria (many with destroyed cristae), short dilated cisterns of granular endoplasmic reticulum and reduced number of ribosome's (reason for lighter color) and normal appearing nucleus. (B) (3-D) cells have normal appearing mitochondria, normal granular endoplasmic reticulum, a cytoplasm dense with ribosomes and a normal nucleus.

ICAM-1 (Fig. 4D) strongly labels endothelial cells. The normal human lung sample is provided as a control and for comparison where the brown stain is located on the basal membrane. Figure 4E (2-D) has no positive response. Figure 4F (3-D) displays positive staining for ICAM-1 (a brown color on the cell surface) on cells even though the cells are not ordered as in Figure 4D.

Markers of cell (epithelial polarity). EMA (MUC1) labels normal secretory epithelium thus determining polarity in normal human lung (Fig. 5A). Figure 5B (2-D) has no positive result, whereas 5C (3-D) displays a strongly positive result located on the cell surface.

Cytokeratin 7 (Fig. 5D) reacts with cytokeratin of epithelial cells and is seen as a brown cytoplasmic staining in the normal lung tissue. Figure 5E (2-D) has a small amount of brown isolated to the cell membrane whereas in Figure 5F once again the brown stain is cytoplasmic (→).

Villin (Fig. 5) labels microvilli, cytoskeletal markers found only in epithelial cells. Of particular interest was the homogeneous positive staining for villin (Table 2) of the 3-D sample and expressed at the surfaces of most areas of the cell/bead aggregates.

Collagen IV (Fig. 5) labels basement membrane and extracellular matrix components and was found to be positive in the control tissue expressed on the cell surface (Fig. 5J). No positive result seen on the 2-D samples (Fig. 5K) whereas there is a positive response in the 3-D samples again at the cell surface (Fig. 5L).

Markers of differentiation. Tubulin, a cytoskeletal marker is labeled as a cytoplasmic protein in differentiated cells as seen in the control sample (Fig. 6A). No positive staining seen in the 2-D (Fig. 6B) sample. Of particular interest was the homogeneous positive staining for tubulin (Table 2) of the 3-D BZR-T33 cells and expressed at the surfaces of most areas of the cell/bead aggregates (Fig. 6C).

VWR/Factor VIII present in the cytoplasm of endothelial cells seen in the control tissue (Fig. 6D). Negative in the 2-D (Fig. 6E) sample and present in the 3-D samples, again as a cytoplasmic brown color.

Hu Mucin is positive as a red color and this antigen labeled the cytoplasm as brown in the normal tissue (Fig. 6G). The 2-D culture (Fig. 6H) does display a red mucin positive response in the extracellular space whereas the 3-D cultures are exhibiting staining for Mucin similar to that of the human tissue is indicative of the degree of the differentiation of the TLA's.

As shown in each of the figures and Table 1, each of the cell specific stains compared more favorably with the 3-D human tissues controls.

Discussion

The goal for this study was to compare the cellular morphology between cells grown in traditional culture systems to that of the same cells grown in a 3-D system. We were able to determine that these transformed lung cells grown under 3-D conditions have demonstrated marker expression more closely related to cells grown in situ rather than those in traditional culture conditions, that cellular ultrastructure is more suggestive of normalcy; and that the 3-D model allowed for identification of these cells migrating through a culture of immortalized lung cells.

This manuscript is the second in a series of manuscripts that is studying the relevance of the 3-D model of culturing cells (normal, immortalized, transfected and primary) in lung cancer. Ideally, cell-based lung models should reproduce the structural organization, multicellular complexity, differentiation state, and function of the human respiratory epithelium. Immortalized human epithelial cell lines, such as BEAS-2B,[18] transformed human epithelial cell lines resulting in a malignant phenotype (BZR-T33),[52] primary normal human bronchial epithelial (NHBE) cells,[53] and primary human carcinomas are used to study pathobiology and therapeutic interventions in lung cancer. Traditional monolayer cultures (2-D) of immortalized human broncho-epithelial (HBE) cells and transformed cells represent homogenous lineages, is convenient with high proliferation rates. Such models, however, lack the morphology (cellular and mass) and the cell-cell and cell-matrix interactions characteristic of human respiratory epithelia in vivo. Their state of differentiation and intracellular signaling pathways differ from epithelial cells because of their non-human growth environment. Primary cell lines of human broncho-epithelial cells and human lung cancers provide a more differentiated model similar to the structure and function of epithelial cells in vivo; however, these models are short-lived in vitro.[53,54]

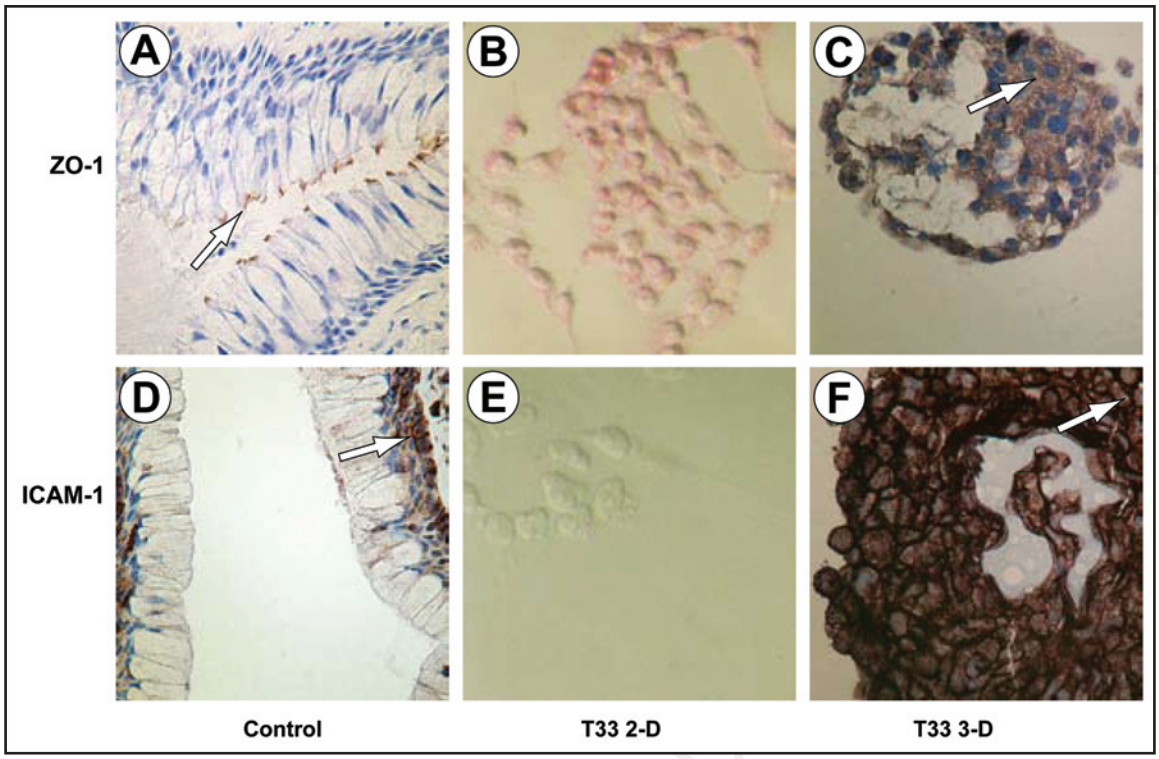

Figure 4. Markers of cell-to-cell junctions. (A) is normal human lung tissue and displays a brown (positive) color at the luminal (apical) border (←). (B) (2-D) has no positive result present, whereas (C) (3-D) shows a strong positive response on cell surfaces. (D) displays a positive response in the normal human lung directed to the basal membrane (→). The 2-D sample (E) has no positive response. In contrast the 3-D sample (F) shows a strong positive reaction to the cell membrane despite the lack to a tissue-like organization. The 3-D aggregates (C and F) show a distinct localization to the cell-cell interface.

True cellular differentiation involves complex cellular interactions,[55-57] in which cell membrane junctions, extracellular matrices (e.g., basement membrane and ground substances) and soluble signals (endocrine, autocrine and paracrine) play important roles.[58-61] This process is also influenced by the spatial relationships (niche) of cells to each other. The responsiveness to exogenous mediators such as cytokines requires more than simply the presence of receptors. Cell communication and signal exchanges through intercellular junctions, paracrine factors and cell adhesion molecules are important to cell morphology and function.[62] Cell-based models are needed that reproduce both the structural organization and multicellular complexity of the human lung while enabling study of therapeutic interventions. Ideally, the differentiation state and function of a human organ should also be simulated for the model to be authentic.

The data presented suggest that the differentiation seen in the 3-D model of a lung cancer from a transformed lung cell line more closely resembles the differentiation seen in a lung cancer tissue than that found in the 2-D model. The presence of large 3-D tissue-like masses of lung cancer cells that express differentiated epithelial and mesenchymal cell markers offers a multitude of possibilities for cell biological investigations. The data are confirmed in Figures 3 (EMs) and 4–6 (IHC), and represent concomitant cellular differentiation marker expression and architectural ordering as compared to normal human tissue. Functional epithelial cell brush borders (Fig. 4) with extracellular matrix and basal lamina components (Fig. 5) represent ordering of tissue and cellular polarity resulting from the molecular and physical conditions of the culture system.

The role of basement membranes and extracellular matrix and their relationship to epithelial-mesenchymal development and differentiation are the subjects of considerable research. Studies indicate that the stromal component exerts a strong and driving influence over developing intestinal mucosa.[63-65] Stallmach et al.[66] have shown that only organ-specific mesenchyme will produce differentiation in epithelium from a given organ site and that embryonic mesenchyme of the same age, but from different organs, are ineffective. Additional information shows that a single fetal epithelial cell type in the last 2–3 days of gestation may express the function of more than one cell, thereby giving rise to DNA synthesis and proliferation.[67,68]

The literature reviewed and the data obtained here would suggest that this model of an oncogenically transformed human lung cell embodies many aspects of differentiation observed in other in vitro and in vivo cell and organ models. Primary distinctions for this model are: (i) the overall scale of the model, (ii) the ability to culture epithelium for long periods without loss of functional cell markers, (iii) to maintain viral production and cellular repair while maintaining the model and (iv) the ability of the system to respond to extensive analyses and manipulations without the termination of a given experiment. Future experiments will study the expression of these markers in malignant lung tissue harvested from patients and when cultured as both 2-D 3-D TLAs and in nude mice. An additional experiment will use the 3-D environment to isolate and characterize lung cancer-initiating stem cells. Another contemplated experiment will use molecular probes and proteomics that will clarify and characterize

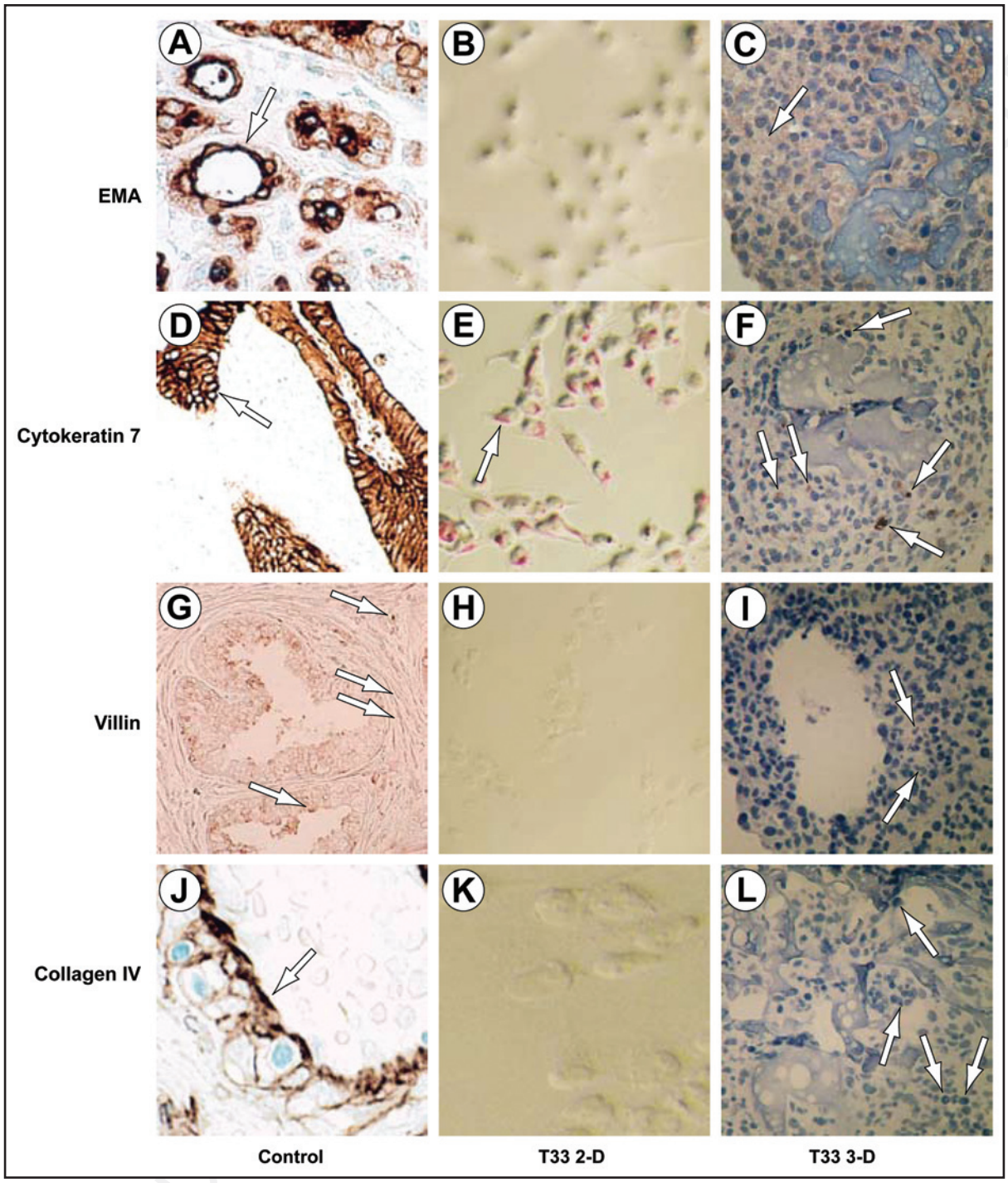

Figure 5. Markers of epithelial cell polarity. EMA (MUC1) labels normal secretory epithelium and is strongly positive in (A) (normal human lung tissue). The positive result (brown) is not present in monolayer cultures (B) whereas it is again strongly positive in the 3-D aggregate culture located to the cell membrane (C). Cytokeratin 7 (D–F) reacts with cytokeratin. Cytokeratin is strongly positive in the cytoplasma of the control tissue (D), minimally present as a stain on the cell surface of the 2-D cells (E) and absent in monolayer cultures (F). Villin labels cytoskeleton markers found only in epithelial cells and is strongly positive in the control normal human lung tissue (G), is nonexistent in the monolayer cultures (H) and diffusely present in the 3-D aggregates (I) being expressed at the surfaces of most areas of cell-bead interfaces. Collagen IV (J–L) labels a major constituent of the basement membrane and is strongly positive in the control (J-normal human lung tissue), is absent in the monolayer section (K) and positive again in (L) the 3-D aggregate section.

the potential of this new model system. Of particular interest will be regulation of unique cytoskeletal proteins such as villin, functional markers such as tubulin, ZO-1, EMA, ICAM-1, a myriad of inflammatory response modifiers, and other markers that may be represented more accurately by large-scale 3-D modeling.

Materials and Methods

Experimental overview. BZR-T33 cells (H-*ras* transfected BEAS-2B) were stably transfected with green fluorescent protein (BZR-T33-GFP). These cells were injected into mice to assay for metastasis. Then BZR-T33 cells (without GFP) were grown in both

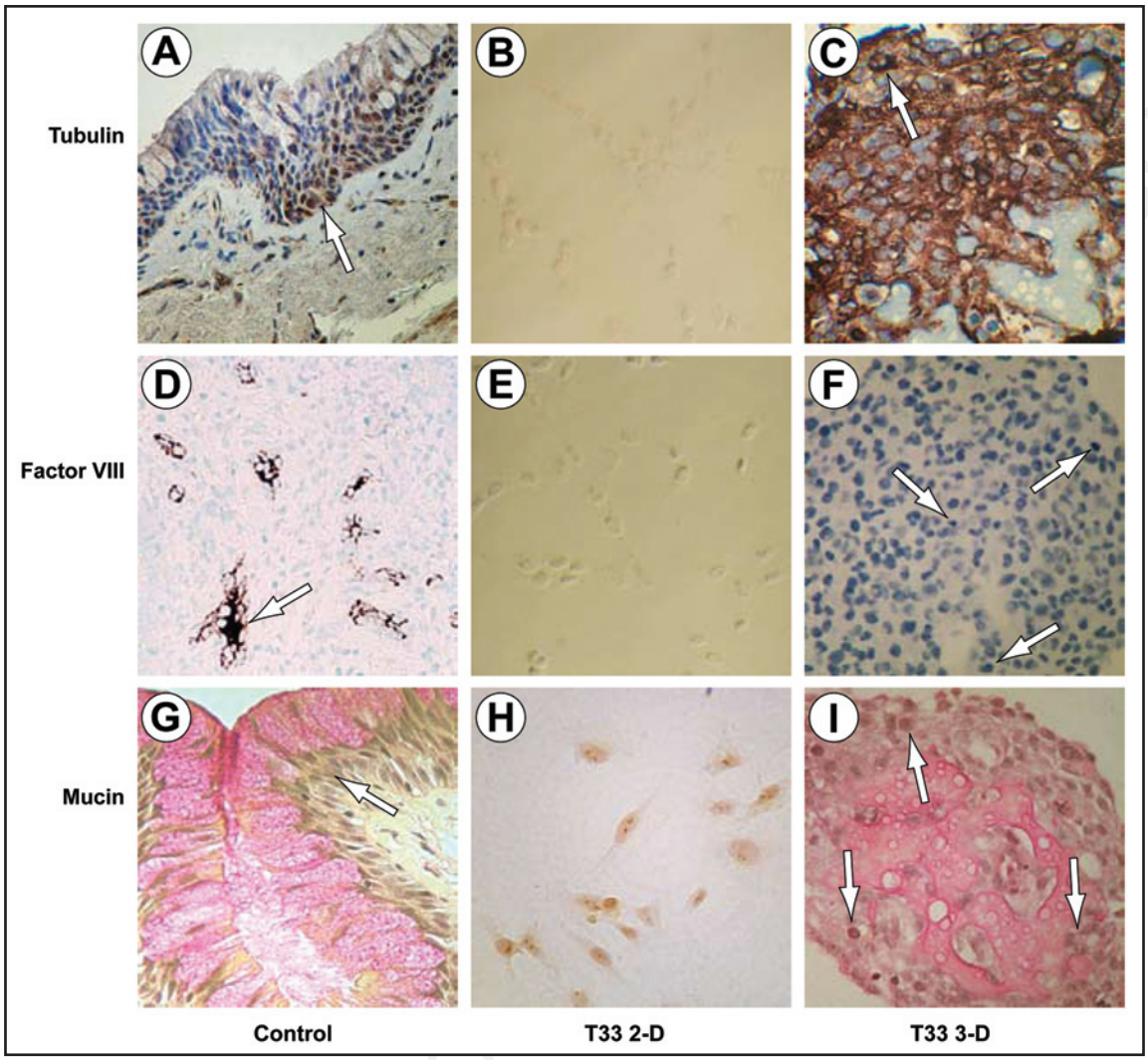

Figure 6. Markers of differentiation. Tubulin (A–C) specific for differentiation is strongly positive in the cytoplasm of control tissue (A-normal human lung tissue), completely absent in the monolayer (B) and again is strongly positive in the cytoplasm of the cells in the 3-D aggregate section (C). VWF (von Willebrand factor) labels a protein present in the cytoplasm of endothelial cells and is strongly positive in the normal human lung sample (D). This antibody expression is totally absent in the 2-D section (E) whereas it is present in the cytoplasm of cells in the 3-D aggregate section (F). Mucin, a normal product of lung cells and is a characteristic of differentiation and is seen as strongly positive in the control sample (G) as a brown color. Section (H) is of the monolayer and is a negative result. Section (I) is from the 3-D aggregates and once again is strongly positive for mucin (brown).

Table 1 **Developmental and differential human immunohistochemistry antibodies**

Antibody	Manufacturer	Dilution
Guinea pig polyclonal anti-ZO-1	abcam, #59724	1:50
Rabbit monoclonal anti-ICAM1 mouse anti-human epithelial	Abcam, #ab53013	1:100
Membrane antigen (EMA also MUC1)	Abcam, #ab49919	1:20
Mouse monoclonal cytokeratin 7	Abcam, #9021	1: 1000
Rabbit polyclonal anti-human villin	Abcam, ab52102	1:50
Collagen IV	Dako #N1536 clone CIV 22	predilute
Tubulin	AbCAm, #ab15246	1:200
Rabbit anti-human Von Willebrand factor	Abcam, #ab6994	1:1000
Mouse monoclonal pan mucin	abcam, #ab736	1:100

Table 2 **Tissue characterization**

Tissue characterization stains	Normal human lung	BZR-T33 2-D	BZR-T33 3-D
ZO-1	3+	1+	4+
EMA	4+	0	2+
ICAM-1	3+	0	4+
Cytokeratin 7	3+	1+	3+
Villin	2+	1+	3+
Collagen IV	4+	2+	4+
Tublin	3+	1+	4+
VWR/Factor VIII	4+	1+	3+
Hu Mucin	4+	1+	4+

the traditional 2-D and the newer 3-D culture environments. Cells were subjected to transmission electron microscopy, and aliquots from both preparations were harvested and stained by IHC for various antibodies. Additionally a co-culture (BZR-T33-GFP cells over a BEAS-2B/HBTC foundation) was developed and assayed by fluorescence microscopy for migration/metastasis of BZR-T33-GFP in vitro.

Cells and cell cultures. Cells were harvested and banked at NASA Johnson Space Center's Laboratory of Cellular Environmental Toxicology and Neurophysiology. Cells were initiated in 2-D monolayer cultures and propagated in GTSF-2 (HyClone Laboratories Inc, Thermo Fisher Scientific, 925 West 1800 South Logan, UT 84321) media supplemented with 10% fetal bovine serum (FBS). All cell cultures were grown in a Forma humidified CO_2 incubator with 95% air and 5% CO_2, and constant atmosphere at a temperature of 37°C. These cell lines are normal mesenchymal cells (human bronchial tracheal cells [HBTC])—obtained from the normal organs of patients, predominantly surgical tissue donors at The University of Texas Medical Branch, Galveston, TX with IRB approval, BEAS-2B—immortalized human bronchial epithelial cell line,[18] and BZR-T33—an H-ras transfectant of BEAS-2B.[18-20] Human lung cells were passaged as required by enzymatic dissociation with a solution of 0.1% trypsin and 0.1% EDTA for five minutes at 37°C. After incubation with the appropriate enzymes, the cells were centrifuged at 1,000 rpm for five minutes in Corning conical 50 ml centrifuge tubes. The cells were then suspended in fresh medium and diluted into T-flasks with 30 ml of fresh growth medium. BEAS-2B epithelial cells were passed as required by dilution at a 1:4 ratio into GTSF-2 medium in T-flasks.[21]

Co-culture experiments. In these experiments BZR-T33 cells were transfected using Lipofectamine Plus™ reagent (cat no. 10964-013, Invitrogen™, *Carlsbad, CA, USA?*). The vector for GFP expression used was pEGFP-N1 vector (Clontech Laboratories Inc., Mountain View, CA, USA). Cells were plated into 6-well plates the day before transfection. For each well of cells to be transfected, 1 μg DNA was diluted into 100 μl medium without serum and then 4 μl plus reagent was added, mixed and incubated at room temperature for 15 minutes. Four μl of diluted LipofectAMINE reagent was added into 100 μl medium without serum in a second tube. DNA-Plus reagent mixture was diluted with LipofectAMINE reagent, mixed and incubated for 15 minutes at room temperature. Medium was replaced on the cells with 0.8 ml serum free medium to which DNA-Plus-LipofectAMINE reagent complex was added to the well. The complexes were mixed into the medium, incubated at 37°C with 5% CO_2 for three hours then 1 ml medium with 10% FBS was added to the cells. The medium was replaced with normal growth medium five hours after the start of transfection. Forty-eight hours after transfection, an additional 800 μg/ml G418 was added into culture medium to select for expression of the transfected G-418 resistance gene.

Animal experiment. Animal experiments were approved by the Animal Care and Use Committee of the University of Texas Medical Branch, Galveston. All animals received humane care in compliance with university guidelines, state and federal regulations, and the standards of the "Guide for the Care and Use of Laboratory Animals," published by the National Institutes of Health (Publication No. 86-23, revised 1985). Eight congenitally athymic nude mice (BALB-C) purchased from Harlan-Sprague Dawley (Indianapolis, IN, USA) were used for this experiment. The mice were matched by sex and were acclimatized for at least two weeks prior to use in a limited-access facility that housed them in laminar-flow racks. At the time of the experiments, animals were approximately six weeks of age.

BZR-T33-GFP cells were grown to 100% confluence in a T-75 flask, harvested in trypsin and collected in 10 ml of media (RPMI 1640). Cell count was determined in Coulter counter in triplicate. Cells were then centrifuged at 5°C x 1,000 rpm x 5 minutes. Approximately 8.5–9 ml media was removed. Concentrated cells were re-suspended and divided to achieve 10^6 cells/100 μL that were then injected subcutaneously in the supraclavicular area. Animals were visualized weekly using a (Charles Beseler Company-Photo Division. CS-21 Stage, Vineland, NJ, Lightools Research, Illumatool-lightsource, SN 2003-709, Encinitas CA, Optronics. Camera System, SN CG602223-PS110, Goleta, CA). Upon completion of the experiment, the animals were euthanized and a complete necropsy performed. Individual organs were inspected for GFP^+ expression by visualization with Beseler Company-Photo Division. CS-21 Stage. Vineland, NJ. Lightools Research. Illumatool-lightsource. SN 2003-709. Encinitas, CA, Optronics. Camera System. SN CG602223-PS110. Goleta, CA). BZR-T33 cells were stably transfected with green fluorescent protein. Visualization of GFP^+ cells by both flow cytometry and photomicroscopy was at 488/515 nm.

Propagation of 3-D cultures. The rotating walled vessel (RWV) is a horizontally rotated transparent culture vessel (Synthecon, Houston, TX USA) with zero head space and center oxygenation. Cells to be cultured in the RWV were initially grown in T-flasks, as described above, in preparation for seeding into the vessels. Normal mesenchymal cells were removed from T-75 (Corning, Corning, NY USA) flasks by enzymatic digestion, washed once with calcium- and magnesium-free phosphate-buffered saline (CMF-PBS), and assayed for viability by trypan blue dye exclusion (Gibco-Invitrogen, Carlsbad, CA USA). Cells were held on ice in fresh growth medium until inoculation. The primary inoculum for each coculture experiment was 2 x 10^5 mesenchymal (HBTC cells) cells/ml in a 55 ml RWV with 5 mg/ml of Cytodex-3 micro carrier beads (Pharmacia, Piscataway, NJ, USA). Cytodex-3 micro carriers were Type I, collagen-coated cyclodextrin beads, 120 microns in diameter. Cultures were allowed to grow for a minimum of 24 to 48 hours before the medium was changed and 2 x 10^5 epithelial cells/ml (BZR-T33-GFP) were added.

Thereafter, fresh medium was replenished by 65% of the total vessel volume each 20 to 24 hours. As metabolic requirements increased, fresh medium was supplemented with an additional 100 mg/dl of glucose. The parameters of glucose utilization and pH were surveyed via iStat^{TM} (I-stat, East Windsor, NJ, USA) clinical blood gas analyzer to determine the relative progress and health of the cultures and the rate of cellular growth and viability. Cells were visualized and photographed using fluorescence microscopy.

Electron microscopy. Samples from the RWV cultures were taken for transmission electron microscopy (TEM) at the same times as those taken for growth kinetics and immunohistochemistry.

Transmission electron microscopy (TEM). EM samples were washed three times 0.1 M sodium cacodylate buffer pH 7.4 (#11652, Electron Microscopy Science, Port Washington, PA, USA) then fixed in a solution of 2.5% glutaraldehyde-formaldehyde in 0.1 M sodium cacodylate buffer (#15949, Electron Microscopy Science, Fort Washington, PA USA)—0.3 M sucrose (Sigma, St. Louis, MO, USA)—1% DMSO (Sigma, St. Louis, MO USA) pH 7.4 (Electron Microscopy Science, Fort Washington, PA, USA) overnight at 4°C. The fixed tissue was washed three times in 0.1 M sodium cacodylate buffer, pH 7.4 buffer, post-fixed stained in 0.1 M tannic acid (# 21700, Electron Microscopy Science, Port Washington, PA, USA) in 0.1 M sodium cacodylate pH 7.4 for three hours at room temperature. The tissue samples were washed three times in buffer, and then fixed again in 1.0 M osmium tetroxide (#19152, Electron Microscopy Science, Port Washington, PA, USA) in cacodylate buffer pH 7.4 for 1.5 hours at room temperature. Samples were dehydrated in a series of graded ethanol, and then embedded in EMbed-812 resin (#14120, Electron Microscopy Science, Port Washington, PA, USA). Samples were sectioned at yellow-silver (700 A), mounted on Ni grids and examined under a JEOL-JEM 1010 transmission electron microscope (JEOL, USA) at 80 kV.

Human lung immunohistochemistry (IHC). Three-D aggregates designated for histological and immunohistological staining were washed three times with gentle agitation in 1x PBS (Gibco-Invitrogen, Carlsbad, CA USA) without magnesium and calcium for five minutes. The gentle washing removed foreign protein residues contributed by the use of the 10% FBS GTSF-2 growth media. The 3-D aggregates were then transferred to 50 ml polystyrene tubes and covered with 10% buffered formalin in PBS (Electron Microscopy Service, Ft. Washington, PA, USA) overnight at 4°C and washed three times in PBS. The assemblies were centrifuged less than 1,000 xg to concentrate the bead-cell assembly after which 1 mL of warm noble agar was added for additional stabilization. Assemblies were paraffin-block embedded by standard methods, light sections cut at 3–5 mm on a microtome (Micron HM315, Walldorf, Germany). All unstained sections were stored at 22°C until stained with haematoxylin and eosin (H&E) or with the panel of differential and developmental membrane receptor antibodies (Table 1). The sections were de-paraffinized by normal procedure, antigen retrieved by protein kinase or citrate and blocked with a normal rabbit or mouse sera—0.5% Tween 20 blocking solution. The primary antibody (as identified in Table 1) diluted in the blocking solution was incubated on sections between 9 and 30 minutes, rinsed with distilled water and conjugated with anti-mouse, goat, or rabbit-horseradish peroxidase 2nd antibody (Dako Envision System, Dako, Carpinteria, CA, USA) applied using an automated immunohistochemical stainer (Dako, Carpinteria, CA, USA). Slides were examined by a Zeiss Axioskop (Hamburg, Germany) microscope and images captured with a Kodak DC 290 Zoom (Rochester, NY, USA) digital camera. Two-dimensional IHC controls were prepared as outlined in Tables 1 and 2.[13,22] Briefly, glass microscope slides (Rite-On, Clay Adams cat. no. 3050) placed in 150 mm Petri dishes (Fisher cat. no. 25030-150) were plated at 1 x 10e^3 cells per ml and allowed to incubate at 35.5°C for 48 hours. Slides were harvested, washed twice with calcium- and magnesium-free PBS (Celox Laboratories Inc., St. Paul, MN, USA), and post fixed with 10% buffered formalin (Electron Microscopy Sciences, Ft. Washington, PA, USA). Slides were stained with the antibodies outlined and visualization was achieved as stated above and scored as per Table 3. For all IHC samples, positive antibody staining, and mucin are visualized as brown (immunoperoxidase), blue (hematoxylin) and pink/yellow (mucicarmine), respectively.

The antibodies used to detect cell-type-specific markers are grouped and shown in Table 1 and described below.

Markers of cell-to-cell junctions. Zonula occludentes (ZO-1) is a peripheral membrane protein located at the cytoplasmic surface of epithelial and endothelial cells. The presence of ZO-1 is a measure of tight junctions, and was surveyed to illuminate intercellular communications.[23,24] The presence of ZO-1 is seen in the upper living cell layers of stratified epithelia and is used by us to demonstrate the presence of these structures and to determine cellular polarity.[25]

ICAM-1 is a 85–110 kDa integral membrane glycoprotein. ICAM1 plays an important role in cell adhesion and signaling and is highly expressed on the surface of endothelial cells. It is valuable for the demonstration of capillaries and neoplasm arising from endothelial cells.[26-28] We use the marker to demonstrate the presence of an important mediator of vascular barrier and regulator of endothelial cell adhesion and migration.

Markers of epithelial cell polarity. Epithelial membrane antigen (EMA) also known as MUC1 is an antibody to a human milk fat globule type I transmembrane protein immunogen present in breast epithelial lesions and a variety of simple and glandular epithelium, including the respiratory tract, pancreas, intestine and endometrial tissue. This antibody can be used to detect presence of epithelial tumors especially prominent in squamous cell carcinomas. EMA is specific for markers for epithelial membrane antigen (Anti-EMA) and is used by us to label normal secretory epithelium.[29-31]

Brush cells are specialized epithelial cells scattered throughout the simple epithelia of the respiratory and alimentary tracts and are identified by the presence of proteins villin and fimbrin that not only stain the apical tuft of microvilli but also label projections emanating from the basolateral surface of these cells. We use the presence of villin to discriminate between brush cells and simple epithelium (which will be labeled with cytokeratin 7, below).[32-35]

Cytokeratin 7, a 54 kD member of the intermediate filament family of proteins and is found primarily in epithelial tissues and especially in brush cells within the respiratory tract.[36-38] Presence of this cytokeratin is used to determine the degree of maturation or differentiation within the epithelium.

Villin is an actin regulatory epithelial cell-specific anti-apoptotic protein. It is associated with the microvillar actin core bundle of

intestinal and renal brush border. Localization of cytokeratin 7 and villin allow for a high level of discrimination between brush cells and simple epithelium. We use this marker to help in identifying respiratory brush border cells.[39]

Anti-Collagen IV is directed against collagen IV, a major constituent of the basement membrane.[32] Cultured microvascular endothelial cells isolated from human dermis were examined for the synthesis of basement membrane specific (type IV) collagen and its deposition in subendothelial matrix.[40] These findings confirm the notion that a substrate of laminin and collagen type IV stimulates the in vitro expression of differentiated smooth muscle traits at a higher level than does a substrate of fibronectin.[41] We used this marker to help identify endothelial cell differentiation.

Markers of differentiation. Anti-α Tubulin mAb is a Rabbit polyclonal antibody directed against α tubulin, which in adult tissues is a specific marker for neurons, although altered patterns of expression are noted in cancer.[42] Tubulin is major building block of microtubules present in the cytoplasm of most eukaryotic cells and function in as structural and mobile elements. The major use of this antibody is for labeling in tissue sections and cell culture which we use to show the presence of differentiation.[43-45]

Anti-VWR reacts with von Willebrand factor present in endothelial cells and in the cytoplasm of megakaryocytes.[46] Endothelial cells form a highly differentiated tissue on the inner surface of blood vessels. One of the typical characteristics is the expression of von Willebrand Factor, a protein that participates in blood coagulation.[47] The antibody may identify tumors derived from endothelial cells and megakaryocytic proliferation. The former designation for von Willebrand factor was factor VIII-related antigen.[48] We selected to use von Willebrand factor to show differentiation and to suggest that the potential for angiogenesis being present.

Anti-hu mucin. Mucin is a normal product of the lung cells whose function is to prevent luminal surfaces from sticking to each other and protection from pathogens. This secreted mucin is gel-forming, small, soluble and are produced by epithelial goblet cells and associated sub mucosal glands.[49] The effects of culture conditions on growth and differentiation of human tracheobronchial epithelial (HTBE) cells have been defined. HTBE cells did not express any mucociliary function (ciliogenesis or mucin secretion) on tissue culture plastic.[50,51] We used mucin to detect the presence of differentiated epithelial cells. This specific antibody (pan Mucin antibody b12) is only located at the MCA (mucin-like carcinoma antigen) producing sites, or secreted into stromal tissues and vessels.

Note

This work is covered by the following US Patents:

2006 MSC-23983-1 PCT, Improved Three-Dimensional Cell To Tissue Development Process

2006 MSC-24164-1, Three-Dimensionally Engineered Normal Human Bronchio-Epithelial Tissue Like Assemblies: Targets for Human Respiratory Viral Infections.

1999 U.S. Patent, 5,858,783

Goodwin TJ, et al. "Production of normal mammalian organ culture using a medium containing MEM-alpha, Leibovitz L-15, glucose galactose fructose."

1998 U.S. Patent 5, 846, 807

Goodwin TJ, "Media compositions for three-dimensional mammalian tissue growth under microgravity culture conditions."

1997 U.S. Patent 5,627,021

Goodwin TJ, et al. Multi-Cellular, "Three-Dimensional Living Mammalian Tissue."

1996 U.S. Patent 5,496,722

Goodwin TJ, et al. "Cultured Normal Mammalian Tissue and Process."

1994 U.S. Patent 5,308,764

Goodwin TJ, et al. "Multi-Cellular Three-Dimensional Living Mammalian Tissue."

1993 MSC-21984-1: "Cultured Normal Mammalian Tissue and Process." U.S. Patent Pending.

1992 U.S. Patent 5,153,132

Goodwin TJ, et al. "Three-Dimensional Coculture Process

1992 MSC-22122-1: "Horizontal Rotating-Wall Vessel Viral Propagation in In Vitro Human Tissue Models"

Acknowledgements

This work has been supported by NASA's Biological Sciences and Applications Division, Contract No. NAS9-17720 and a grant from Thermasoltions Inc., of Melbourne, FL, UTMB #58699.

The authors would like to acknowledge the efforts of Eileen Figueroa and Steve Schuenke for their assistance in preparing this manuscript.

References

1. Edelmann M, Gamarra F, da Silva AK, Hornung V, Castro M, Passlick B, et al. Cell cycle effects of radiation on human bronchial epithelium and lung carcinoma cells in monolayer cultures and a three-dimensional co-culture system. Radiat Res 2005; 164:391-9.
2. Fjellbirkeland L, Bjerkvig R, Laerum OD. Non-small-cell lung carcinoma cells invade human bronchial mucosa in vitro. In Vitro Cell Dev Biol Anim 1998; 34:333-40.
3. Olive KP, Tuveson DA. The use of targeted mouse models for preclinical testing of novel cancer therapeutics. Clin Cancer Res 2006; 12:5277-87.
4. Vertrees RA, Deyo DJ, Quast M, Lightfoot KM, Boor PJ, Zwischenberger JB. Development of a human to murine orthotopic xenotransplanted lung cancer model. J Invest Surg 2000; 13:349-58.
5. Vertrees RA, Zwischenberger JB, Boor PJ, Popov V, McCarthy M, Solley TN, et al. Cellular differentiation in three-dimensional lung cell cultures. Cancer Biol Ther 2007; 3:404-12.
6. Hoffman RM. The three-dimensional question: Can clinically relevant tumor drug resistance be measured in vitro? Cancer Metastasis Rev 1994; 13:169-73.
7. Miller MS, Leone-Kabler S, Rollins LA, Wessner LL, Fan M, Schaeffer DO, et al. Molecular pathogenesis of transplacentally induced mouse lung tumors. Exp Lung Res 1998; 24:557-77.
8. Glasser SW, Nogee LM. Genetically engineered mice in understanding the basis of neonatal lung disease. Semin Perinatol 2006; 30:341-9.
9. Kim JB. Three-dimensional tissue culture models in cancer biology. Semin Cancer Biol 2005; 15:365-77.
10. Al-Batran SE, Astner ST, Supthut M, Gamarra F, Brueckner K, Welsch U, et al. Three-dimensional in vitro cocultivation of lung carcinoma cells with human bronchial organ culture as a model for bronchial carcinoma. Am J Respir Cell Mol Biol 1999; 21:200-8.
11. Goodwin TJ, Prewett TL, Spaulding GF, Becker JL. Three-dimensional culture of a mixed mullerian tumor of the ovary: Expression of in vivo characteristics. In Vitro Cell Dev Biol 1997; 33:366-74.
12. Schwarz RP, Goodwin TJ, Wolf DA. Cell culture for three-dimensional modeling in rotating-wall vessels: An application of simulated microgravity. J Tiss Cult Meth 1992; 14:51-8.
13. Goodwin TJ, Prewett TL, Wolf DA, Spaulding GF. Reduced shear stress: A major component in the ability of mammalian tissues to form three-dimensional assemblies in simulated microgravity. J Cell Biochem 1993; 51:301-11.
14. Nickerson CA, Goodwin TJ, Terlonge J, Ott CM, Buchanan KL, Uicker WC, et al. Three-dimensional tissue assemblies: Novel models for the study of Salmonella enterica serovar Typhimurium pathogenesis. Infect Immun 2001; 69:7106-20.
15. Goodwin TJ, Coate-Li L, Linnehan RM, Hammond TG. Selected contribution: A three-dimensional model for assessment of in vitro toxicity in balaena mysticetus renal tissue. J Appl Physiol 2000; 89:2508-17.
16. Goodwin TJ, Jessup JM, Wolf DA. Morphologic differentiation of colon carcinoma cell lines HT-29 and HT-29KM in rotating-wall vessels. In Vitro Cell Dev Biol 1992; 28:47-60.
17. Wang R, Xu J, Juliette L, Castilleja A, Love J, Sung SY, et al. Three-dimensional co-culture models to study prostate cancer growth, progression and metastasis to bone. Semin Cancer Biol 2005; 15:353-64.

18. Ke Y, Reddel RR, Gerwin BI, Miyashita M, McMenamin M, Lechner JF, et al. Human bronchial epithelial cells with integrated SV40 virus T antigen genes retain the ability to undergo squamous differentiation. Differentiation 1988; 38:60-6.
19. Pfeifer AM, Lechner JF, Masui T, Reddel RR, Mark GE, Harris CC. Control of growth and squamous differentiation in normal human bronchial epithelial cells by chemical and biological modifiers and transferred genes. Environ Health Perspect 1989; 80:209-20.
20. Pfeifer AM, Mark GE 3rd, Malan-Shibley L, Graziano S, Amstad P, Harris CC. Cooperation of c-raf-1 and c-myc protooncogenes in the neoplastic transformation of simian virus 40 large tumor antigen-immortalized human bronchial epithelial cells. Proc Natl Acad Sci USA 1989; 86:10075-9.
21. Lelkes PI, Ramos E, Nikolaychik VV, Wankowski DM, Unsworth BR, Goodwin TJ. GTSF-2: A new, versatile cell culture medium for diverse normal and transformed mammalian cells. In Vitro Cell Dev Biol Anim 1997; 33:344-51.
22. Schwarz RP, Goodwin TJ, Wolf DA. Cell culture for three-dimensional modeling in rotating-wall vessels: An application of simulated microgravity. J Tissue Cult Methods 1992; 14:51-7.
23. Tsarfaty I, Rong S, Resau JH, Rulong S, da Silva PP, Vande Woude GF. The Met protooncogene mesenchymal to epithelial cell conversion. Science 1994; 263:98-101.
24. Morita K, Itoh M, Saitou M, Ando-Akatsuka Y, Furuse M, Yoneda K, et al. Subcellular distribution of tight junction-associated proteins (occludin, ZO-1, ZO-2) in rodent skin. J Invest Dermatol 1998; 110:862-6.
25. Langbein L, Grund C, Kuhn C, Praetzel S, Kartenbeck J, Brandner JM, et al. Tight junctions and compositionally related junctional structures in mammalian stratified epithelia and cell cultures derived therefrom. Eur J Cell Biol 2002; 81:419-35.
26. Ohsawa M, Naka N, Tomita Y, Kawamori D, Kanno H, Aozasa K. Use of immunohistochemical procedures in diagnosing angiosarcoma. Evaluation of 98 cases. Cancer 1995; 75:2867-74.
27. Wang Y, Sheibani N. PECAM-1 isoform-specific activation of MAPK/ERKs and small GTPases: Implications in inflammation and angiogenesis. J Cell Biochem 2006; 98:451-68.
28. Kondo S, Scheef EA, Sheibani N, Sorenson CM. PECAM-1 isoform-specific regulation of kidney endothelial cell migration and capillary morphogenesis. Am J Physiol Cell Physiol 2007; 292:2070-83.
29. Pinkus GS, Kurtin PJ. Epithelial membrane antigen—A diagnostic discriminant in surgical pathology: Immunohistochemical profile in epithelial, mesenchymal and hematopoietic neoplasms using paraffin sections and monoclonal antibodies. Hum Pathol 1985; 16:929-40.
30. Heyderman E, Strudley I, Powell G, Richardson TC, Cordell JL, Mason DY. A new monoclonal antibody to epithelial membrane antigen (EMA)-E29. A comparison of its immunocytochemical reactivity with polyclonal anti-EMA antibodies and with another monoclonal antibody, HMFG-2. Br J Cancer 1985; 52:355-61.
31. Saad RS, Cho P, Liu YL, Silverman JF. The value of epithelial membrane antigen expression in separating benign mesothelial proliferation from malignant mesothelioma: A comparative study. Diagn Cytopathol 2005; 32:156-9.
32. Odermatt BF, Lang AB, Ruttner JR, Winterhalter KH, Trueb B. Monoclonal antibodies to human type IV collagen: Useful reagents to demonstrate the heterotrimeric nature of the molecule. Proc Natl Acad Sci USA 1984; 81:7343-7.
33. Nusrat A, Delp C, Madara JL. Intestinal epithelial restitution. Characterization of a cell culture model and mapping of cytoskeletal elements in migrating cells. J Clin Invest 1992; 89:1501-11.
34. Hofer D, Drenckhahn D. Cytoskeletal markers allowing discrimination between brush cells and other epithelial cells of the gut including enteroendocrine cells. Histochem Cell Biol 1996; 105:405-12.
35. Brown D, Lee R, Bonventre JV. Redistribution of villin to proximal tubule basolateral membranes after ischemia and reperfusion. Am J Physiol 1997; 273:1003-12.
36. Moll R, Franke WW, Schiller DL, Geiger B, Krepler R. The catalog of human cytokeratins: patterns of expression in normal epithelia, tumors and cultured cells. Cell 1982; 31:11-24.
37. Kasper M, Hofer D, Woodcock-Mitchell J, Migheli A, Attanasio A, Rudolf T, et al. Colocalization of cytokeratin 18 and villin in type III alveolar cells (brush cells) of the rat lung. Histochemistry 1994; 101:57-62.
38. Wells MJ, Hatton MW, Hewlett B, Podor TJ, Sheffield WP, Blajchman MA. Cytokeratin 18 is expressed on the hepatocyte plasma membrane surface and interacts with thrombin-antithrombin complexes. J Biol Chem 1997; 272:28574-81.
39. Wang Y, Srinivasan K, Siddiqui MR, George SP, Tomar A, Khurana S. A novel role for villin in intestinal epithelial cell survival and homeostasis. J Biol Chem 2008; 14:9454-64.
40. Kramer RH, Fuh GM, Karasek MA. Type IV collagen synthesis by cultured human microvascular endothelial cells and its deposition into the subendothelial basement membrane. Biochemistry 1985; 24:7423-30.
41. Thyberg J, Hultgardh-Nilsson A. Fibronectin and the basement membrane components laminin and collagen type IV influence the phenotypic properties of subcultured rat aortic smooth muscle cells differently. Cell Tissue Res 1994; 276:263-71.
42. Katsetos CD, Herman MM, Mork SJ. Class III beta-tubulin in human development and cancer. Cell Motil Cytoskeleton 2003; 55:77-96.
43. Dettman RW, Turner FR, Hoyle HD, Raff EC. Embryonic expression of the divergent Drosophila beta3-tubulin isoform is required for larval behavior. Genetics 2001; 158:253-63.
44. Draberova E, Lukas Z, Ivanyi D, Viklicky V, Draber P. Expression of class III beta-tubulin in normal and neoplastic human tissues. Histochem Cell Biol 1998; 109:231-9.
45. Dumontet C, Isaac S, Souquet PJ, Bejui-Thivolet F, Pacheco Y, Peloux N, et al. Expression of class III beta tubulin in non-small cell lung cancer is correlated with resistance to taxane chemotherapy. Bull Cancer 2005; 92:25-30.
46. Jones TR, Kao KJ, Pizzo SV, Bigner DD. Endothelial cell surface expression and binding of factor VIII/von Willebrand factor. Am J Pathol 1981; 103:304-8.
47. Hohenwarter O, Schmatz C, Katinger H. Stability of von Willebrand factor secretion in different human endothelial hybrid cell lines. Cytotechnology 1992; 8:31-7.
48. Sehested M, Hou-Jensen K. Factor VII related antigen as an endothelial cell marker in benign and malignant diseases. Virchows Arch A Pathol Anat Histol 1981; 391:217-25.
49. Russo CL, Spurr-Michaud S, Tisdale A, Pudney J, Anderson D, Gipson IK. Mucin gene expression in human male urogenital tract epithelia. Hum Reprod 2006; 21:2783-93.
50. Wu R, Martin WR, Robinson CB, St. George JA, Plopper CG, Kurland G, et al. Expression of mucin synthesis and secretion in human tracheobronchial epithelial cells grown in culture. Am J Respir Cell Mol Biol 1990; 3:467-78.
51. Bernacki SH, Nelson AL, Abdullah L, Sheehan JK, Harris A, Davis CW, et al. Mucin gene expression during differentiation of human airway epithelia in vitro. Muc4 and muc5b are strongly induced. Am J Respir Cell Mol Biol 1999; 20:595-604.
52. Bonfil RD, Reddel RR, Ura H, Reich R, Fridman R, Harris CC, et al. Invasive and metastatic potential of a v-Ha-ras-transformed human bronchial epithelial cell line. J Natl Cancer Inst 1989; 81:587-94.
53. Stoner GD, Katoh Y, Foidart JM, Myers GA, Harris CC. Identification and culture of human bronchial epithelial cells. Methods Cell Biol 1980; 21:15-35.
54. Gray GD, Wickstrom E. Evaluation of anchorage-independent proliferation in tumorigenic cells using the redox dye alamarBlue. Biotechniques 1996; 21:780.
55. Wiens D, Park CS, Stockdale FE. Milk protein expression and ductal morphogenesis in the mammary gland in vitro: Hormone-dependent and -independent phases of adipocyte-mammary epithelial cell interaction. Dev Biol 1987; 120:245-58.
56. Fukamachi H. Disorganization of stroma alters epithelial differentiation of the glandular stomach in adult mice. Cell Tissue Res 1986; 243:65-8.
57. Sutherland RM. Cell and environment interactions in tumor microregions: the multicell spheroid model. Science 1988; 240:177-84.
58. Kaye GI, Siegel LF, Pascal RR. Cell replication of mesenchymal elements in adult tissues I. The replication and migration of mesenchymal cells in the adult rabbit dermis. Anat Rec 1971; 169:593-611.
59. Buset M, Winawer S, Friedman E. Defining conditions to promote the attachment of adult human colonic epithelial cells. In Vitro Cell Dev Biol 1987; 23:403-12.
60. Daneker GW Jr, Mercurio AM, Guerra L, Wolf B, Salem RR, Bagli DJ, et al. Laminin expression in colorectal carcinomas varying in degree of differentiation. Arch Surg 1987; 122:1470-4.
61. Durban EM, Knepper JE, Medina D, Butel JS. Influence of mammary cell differentiation on the expression of proteins encoded by endogenous BALB/c mouse mammary tumor virus genes. Virus Res 1990; 16:307-23.
62. Clissi B, D'Ambrosio D, Geginat J, Colantonio L, Morrot A, Freshney NW, et al. Chemokines fail to upregulate beta1 integrin-dependent adhesion in human Th2 T lymphocytes. J Immunol 2000; 164:3292-300.
63. Haffen K, Kedinger M, Simon-Assmann P. Mesenchyme-dependent differentiation of epithelial progenitor cells in the gut. J Pediatr Gastroenterol Nutr 1987; 6:14-23.
64. Kedinger M, Haffen K, Simon-Assmann P. Intestinal tissue and cell cultures. Differentiation 1987; 36:71-85.
65. Kedinger M, Simon-Assmann P, Alexandre E, Haffen K. Importance of a fibroblastic support for in vitro differentiation of intestinal endodermal cells and for their response to glucocorticoids. Cell Differ 1987; 20:171-82.
66. Stallmach A, Hahn U, Merker HJ, Hahn EG, Riecken EO. Differentiation of rat intestinal epithelial cells is induced by organotypic mesenchymal cells in vitro. Gut 1989; 30:959-70.
67. Quaroni A. Expression of YBB 3/10 antigen in human tumor colon cell lines and its induction by N,N-dimethylformamide. J Natl Cancer Inst 1985; 74:591-602.
68. Quaroni A, Isselbacher KJ. Study of intestinal cell differentiation with monoclonal antibodies to intestinal cell surface components. Dev Biol 1985; 111:267-79.